NUSC Technical Report 8943
18 September 1991

Analytical Evaluation of a Flush-Mounted Hydrophone Array Response to a Modified Corcos Turbulent Wall Pressure Spectrum

Sung H. Ko
Submarine Sonar Department

Naval Underwater Systems Center
Newport, Rhode Island • New London, Connecticut

Preface

This report was prepared under NUSC Project No. A19040, "Hull Array Improvement Project." The NUSC Project Managers were Dr. Howard H. Schloemer (Code 2133) and Frank A. Tito (Code 2131); the Principal Investigators of the Large Area Array Modeling Program were Dr. Howard H. Schloemer and Dr. Sung H. Ko (Code 2133). The Sponsoring Activity is the Naval Sea Systems Command (Code 06UR).

The technical reviewers for this report were Dr. Howard H. Schloemer (Code 2133) and Dr. Albert H. Nuttall (Code 304).

The author would like to express his appreciation to Dr. Howard H. Schloemer and Dr. Albert H. Nuttall for their helpful discussions.

Reviewed and Approved: 18 September 1991

F. J. Kingsbury

Dr. F. J. Kingsbury
Head, Submarine Sonar Department

REPORT DOCUMENTATION PAGE

Form Approved
OMB No. 0704-0188

1. AGENCY USE ONLY (Leave blank)	2. REPORT DATE	3. REPORT TYPE AND DATES COVERED
	18 September 1991	Progress Nov. 1990 to Sept. 1991

4. TITLE AND SUBTITLE
Analytical Evaluation of a Flush-Mounted Hydrophone Array Response to a Modified Corcos Turbulent Wall Pressure Spectrum

5. FUNDING NUMBERS
PE: 63504
SPR: S0223

6. AUTHOR(S)
Sung H. Ko

7. PERFORMING ORGANIZATION NAME(S) AND ADDRESS(ES)
Naval Underwater Systems Center
New London, CT 06320

8. PERFORMING ORGANIZATION REPORT NUMBER
NUSC
TR 8943

9. SPONSORING/MONITORING AGENCY NAME(S) AND ADDRESS(ES)
Naval Sea Systems Command
Washington, DC 20362-5105

10. SPONSORING/MONITORING AGENCY REPORT NUMBER

11. SUPPLEMENTARY NOTES

12a. DISTRIBUTION/AVAILABILITY STATEMENT
Approved for public release;
distribution is unlimited.

12b. DISTRIBUTION CODE

13. ABSTRACT *(Maximum 200 words)*

This report describes the analytical evaluation of the performance of an array of rectangular hydrphones mounted on a rigid surface in the reduction of flow noise, using a modified Corcos. This report also compares the results obtained from the modified Corcos model with those calculated for the original Corcos model. Mathematical details that follow the procedure described in an earlier work are given for the evaluation of the frequency spectral density. This work provides a tool for a quick estimate on the response of an array of hydrophones to turbulent boundary layer pressure fluctuations.

14. SUBJECT TERMS		15. NUMBER OF PAGES
Arrays	Noise Reduction	40
Hydrophone	Planar Array	16. PRICE CODE
Noise Level	Turbulent Boundary Layer	

17. SECURITY CLASSIFICATION OF REPORT	18. SECURITY CLASSIFICATION OF THIS PAGE	19. SECURITY CLASSIFICATION OF ABSTRACT	20. LIMITATION OF ABSTRACT
UNCLASSIFIED	UNCLASSIFIED	UNCLASSIFIED	SAR

NSN 7540-01-280-5500

TABLE OF CONTENTS

LIST OF ILLUSTRATIONS

LIST OF TABLES

ANALYTICAL EVALUATION OF A FLUSH-MOUNTED HYDROPHONE ARRAY RESPONSE TO A MODIFIED CORCOS TURBULENT WALL PRESSURE SPECTRUM

INTRODUCTION

The purpose of this work is to evaluate analytically the performance of an array of rectangular hydrophones mounted on a rigid surface in reducing flow noise, using a modified Corcos model, and to compare the results calculated for the modified Corcos model with those obtained for the original Corcos model.

The analytical model used in the present work is an array of rectangular hydrophones flush-mounted on a rigid surface and exposed to turbulent flow. The mathematical development for this type of problem has been described by Ko and Nuttall.[1] An approximate technique has been developed by Thompson[2] to perform the rapid evaluation of power spectral density integrals. In the present work, the technique developed in reference 1 has been extended to the evaluation of the array response to a modified Corcos turbulent wall pressure spectrum. Using the original Corcos model, the extensive calculation of the flow induced noise

received by a rectangular hydrophone embedded in a layer of elastomer backed by a rigid surface was made by Ko and Schloemer.[3] Further calculations of turbulent boundary layer pressure fluctuations received by an array of rectangular hydrophones embedded within the elastomer layer backed by an elastic plate with a finite thickness were made by Ko and Schloemer.[4]

An analytical development for determination of the frequency spectral density that gives the response of a hydrophone array mounted on a rigid surface to turbulent boundary layer pressure fluctuations is presented. The double integral that represents the frequency spectral density is replaced by the product of two single integrals. The evaluation of the single integral is based on the contour integral (residue) method. Numerically integrated results compare favorably with the results calculated using the exact expression presented here.

This report presents mathematical details for the evaluation of the frequency spectral density and then provides calculations of turbulent boundary layer noise reductions, which are given relative to the noise level calculated for a point hydrophone. The frequency spectral density is expressed in $dB//\mu Pa^2 Hz^{-1}$. A number of parametric studies to provide hydrophone array design guidelines for a quick estimate of their performance is presented. Calculated results were compared with those obtained using the original Corcos model.

THEORETICAL ANALYSIS

The response of an array of rectangular hydrophones flush-mounted on a planar, rigid surface to turbulent boundary layer pressure fluctuations can be calculated theoretically from the frequency spectral density (figures 1 and 2):

$$Q(\omega) = 2\pi \int_{-\infty}^{+\infty}\int P(k_x,k_y,\omega)\, S(k_x,k_y)\, A(k_x,k_y)\, dk_x dk_y \ , \qquad (1)$$

where $Q(\omega)$ is the frequency spectral density, $P(k_x,k_y,\omega)$ is the turbulent wall pressure spectrum, $S(k_x,k_y)$ is the rectangular hydrophone function, $A(k_x,k_y)$ is the rectangular array function, $\omega=2\pi f$ is the angular frequency in rad/s, f is the frequency in Hz, and k_x and k_y are the wavenumbers in the x- and y-directions, respectively. The turbulent wall pressure spectrum used in the present study, a modified Corcos model, is as follows:[5]

$$P(k_x,k_y,\omega) = \frac{a_o\, \rho_o^2\, v_*^4}{\omega\, \pi^2} \left\{ \frac{c_1\, k_c}{(k_x - k_c)^2 + (c_1 k_c)^2} \ \frac{c_2\, k_c}{k_y^2 + (c_2 k_c)^2} \right\}$$

$$\times \left\{ 1 + \frac{(c_1 k_c)^2 - (k_x - k_c)^2}{(c_1 k_c)^2 + (k_x - k_c)^2} \right\}$$

$$= \frac{P(o,\omega)}{\pi^2} \left\{ \frac{2\,(c_1 k_c)^3}{[(k_x - k_c)^2 + (c_1 k_c)^2]^2} \ \frac{c_2 k_c}{k_y^2 + (c_2 k_c)^2} \right\} \ , \qquad (2)$$

where $k_c = \omega/u_c$ is the convective wavenumber, and u_c is the convective flow speed. The point power spectrum $P(o,\omega)$ is given by

$$P(o,\omega) = a_o \rho_o^2 v_*^4/\omega \ , \tag{3}$$

where a_o, c_1 and c_2 are the constants to be determined, ρ_o is the fluid density, and v_* is the friction velocity which is defined as

$$v^* = (\tau_o/\rho_o)^{1/2}, \tag{4}$$

where τ_o is the wall shear stress. Using the definition of the skin friction coefficient, one may write the friction velocity as

$$v_* = (c_f/2)^{1/2} U, \tag{5}$$

where c_f is the skin friction coefficient. Schlichting[6] suggested the following expression for c_f by fitting the relation between the friction coefficient c_f and the Reynolds number R_x,

$$c_f = 0.455 \ (\log R_x)^{-2.58} \ . \tag{6}$$

An array of rectangular hydrophones is depicted in figure 2. The rectangular hydrophone and array functions are given by

$$S(k_x,k_y) = \left[\frac{\sin(k_xL_x/2)}{k_xL_x/2} \times \frac{\sin(k_yL_y/2)}{k_yL_y/2}\right]^2 , \qquad (7)$$

and

$$A(k_x,k_y) = \left[\frac{\sin(N_xk_xd_x/2)}{N_x \sin(k_xd_x/2)} \times \frac{\sin(N_yk_yd_y/2)}{N_y \sin(k_yd_y/2)}\right]^2 , \qquad (8)$$

where L_x and L_y are the dimensions of the rectangular hydrophone, d_x and d_y are the central distances between adjacent hydrophones of the array, and N_x and N_y are the numbers of hydrophones in the x- and y-directions, respectively.

If equations (2), (7), and (8) are substituted into equation (1), then equation (1) is conveniently rewritten as

$$Q(\omega) = 2\pi \{ P_o(\omega)\, Q_x(\omega)\, Q_y(\omega) \} , \qquad (9)$$

where

$$P_o(\omega) = 2a_o\rho_o{}^2v_*{}^4 (c_1k_c)^3 (c_2k_c)/(\pi^2\omega) , \qquad (10)$$

$$Q_x(\omega) = \int_{-\infty}^{+\infty} \frac{1}{\left[(k_x-k_c)^2+(c_1k_c)^2\right]^2} \left[\frac{\sin(k_xL_x/2)}{k_xL_x/2}\right]^2 \times \left[\frac{\sin(N_xk_xd_x/2)}{N_x \sin(k_xd_x/2)}\right]^2 dk_x , \qquad (11)$$

and

$$Q_y(\omega) = \int_{-\infty}^{+\infty} \frac{1}{k_y^2 + (c_2 k_c)^2} \left[\frac{\sin(k_y L_y/2)}{k_y L_y/2}\right]^2 \times \left[\frac{\sin(N_y k_y d_y/2)}{N_y \sin(k_y d_y/2)}\right]^2 dk_y \ . \qquad (12)$$

For the convenience of the ensuing mathematical manipulations, let us define new variables

$$\begin{aligned} x &= k_x \ , \\ y &= k_y \ , \\ \zeta &= k_c \ , \\ \alpha &= c_1 k_c \ , \\ \beta &= c_2 k_c \ , \\ a &= L_x/2 \ , \\ b &= L_y/2 \ , \\ M &= N_x \ , \\ N &= N_y \ , \\ d &= d_x/2 \ , \text{ and} \\ e &= d_y/2 \ . \end{aligned} \qquad (13)$$

Note that x and y are used as dummy variables for the purpose of integration.

Then, using the parameters defined in equation (13), equation (10) is rewritten as

$$P_o(\omega) = 2a_o \rho_o^2 v_*^4 \ \alpha^3 \beta/(\pi^2 \omega). \qquad (14)$$

RESPONSE OF A POINT HYDROPHONE

Using the parameters defined in equation (13), the response of a point hydrophone is written as

$$Q(\omega) = 2\pi\, P_o(\omega) \int_{-\infty}^{+\infty} \frac{dx}{\left[(x-\zeta)^2 + \alpha^2\right]^2} \int_{-\infty}^{+\infty} \frac{dy}{y^2 + \beta^2} \,. \tag{15}$$

To evaluate the first integral in equation (15), let $x'=x-\zeta$; then

$$I_1 \equiv \int_{-\infty}^{+\infty} \frac{dx'}{\left[x'^2 + \alpha^2\right]^2} \,. \tag{16}$$

The integrated value of equation (16) can be obtained by evaluating the following contour integral:

$$\left\{ \int_{\Gamma} + \int_{-R}^{+R} \right\} f(z)\, dz = 2\pi i\, (\mathrm{Res})_{z=i\alpha} \,, \tag{17}$$

where $z=x'+iy$ (figure 3) and $(\mathrm{Res})_{z=i\alpha}$ is the residue of the function $f(z)=1/(z^2+\alpha^2)^2$ at $z=i\alpha$. By Jordan's lemma, the first integral in equation (17) becomes zero as $R\to\infty$, and the residue of $f(z)$ at $z=i\alpha$ is obtained as

$$(\text{Res})_{z=i\alpha} = \frac{1}{(2-1)!}\frac{d}{dz}\left\{ (z-i\alpha)^2 f(z) \right\}_{z=i\alpha}$$

$$= \frac{d}{dz}\left\{ \frac{1}{(z+i\alpha)^2} \right\}_{z=i\alpha} = \frac{1}{4i\alpha^3} \quad . \tag{18}$$

Then,

$$I_1 = 2\pi i \ (\text{Res})_{z=i\alpha} = \pi/(2\alpha^3). \tag{19}$$

Similarly, one obtains the second integral in equation (15) as follows:

$$J_1 = \int_{-\infty}^{+\infty} \frac{dy}{y^2 + \beta^2} = \frac{\pi}{\beta} \ . \tag{20}$$

Then, the frequency spectral density calculated for a point hydrophone is written as

$$Q(\omega) = 2\pi \ P_o(\omega) \ I_1 \ J_1$$
$$= 2\pi \ a_o \ \rho_o^2 \ v_*^4/\omega. \tag{21}$$

RESPONSE OF AN ARRAY OF FINITE HYDROPHONES

Using the parameters defined in equation (13), the response of an array of hydrophones to turbulent boundary layer pressure fluctuations is written as

$$Q(\omega) = 2\pi P_o(\omega) \int_{-\infty}^{+\infty} \frac{1}{\left[(x-\zeta)^2+\alpha^2\right]^2} \left[\frac{\sin(ax)}{ax}\right]^2 \left[\frac{\sin(Mdx)}{M \sin(dx)}\right]^2 dx$$

$$\times \int_{-\infty}^{+\infty} \frac{1}{y^2+\beta^2} \left[\frac{\sin(by)}{by}\right]^2 \left[\frac{\sin(Ney)}{N \sin(ey)}\right]^2 dy \ . \qquad (22)$$

To evaluate the first integral in equation (22), let $x'=x-\zeta$; then

$$I_2 \equiv \frac{1}{a^2M^2} \int_{-\infty}^{+\infty} \frac{\sin^2[a(x'+\zeta)] \sin^2[Md(x'+\zeta)]}{(x'+\zeta)^2(x'^2+\alpha^2)^2 \sin^2[d(x'+\zeta)]} dx' \ . \qquad (23)$$

The last term in equation (23) can be expressed in a series:

$$\frac{\sin[Md(x'+\zeta)]}{\sin[d(x'+\zeta)]} = \sum_{m=0}^{M-1} \exp\{id(x'+\zeta)(2m+1-M)\}$$

$$= \sum_{m=0}^{M-1} \exp\{-id(x'+\zeta)(2m+1-M)\} \ . \qquad (24)$$

Then,

$$\frac{\sin^2[Md(x'+\zeta)]}{\sin^2[d(x'+\zeta)]} = \sum_{\substack{m=0 \\ n=0}}^{M-1} \exp\{2id(m-n)(x'+\zeta)\} \ . \qquad (25)$$

If equation (25) is substituted into equation (23), then equation (23) is written as

$$I_2 = \mathrm{Re}\ \frac{1}{a^2M^2} \sum_{\substack{m=0\\n=0}}^{M-1} \int_{-\infty}^{+\infty} \frac{\sin^2[a(x'+\zeta)]}{(x'+\zeta)^2(x'^2+\alpha^2)^2} \exp[2i|m-n|d(x'+\zeta)]\, dx'$$

$$= \frac{1}{2a^2M^2} \sum_{\substack{m=0\\n=0}}^{M-1} \int_{-\infty}^{+\infty} \frac{\{1-\cos[2a(x'+\zeta)]\}\ \cos\{2d|m-n|(x'+\zeta)\}}{(x'+\zeta)^2(x'^2+\alpha^2)^2}\, dx'$$

$$= \frac{1}{2a^2M^2} \sum_{\substack{m=0\\n=0}}^{M-1} \left\{ \int_{-\infty}^{+\infty} \frac{\cos[2d|m-n|(x'+\zeta)]}{(x'+\zeta)^2\ (x'^2+\alpha^2)^2}\, dx' \right.$$

$$- \frac{1}{2} \int_{-\infty}^{+\infty} \frac{\cos[2(a+d|m-n|)(x'+\zeta)]}{(x'+\zeta)^2\ (x'^2+\alpha^2)^2}\, dx'$$

$$\left. - \frac{1}{2} \int_{-\infty}^{+\infty} \frac{\cos[2(a-d|m-n|)(x'+\zeta)]}{(x'+\zeta)^2\ (x'^2+\alpha^2)^2}\, dx' \right\} . \qquad (26)$$

The three integrals shown in the brace of equation (26) can be evaluated by considering the general form

$$f(z) = \frac{\exp(2i\beta_o(z+\zeta))}{(z+\zeta)^2\ (z^2+\alpha^2)^2} , \qquad (27)$$

where $z=x'+iy$ (figure 4), $\beta_o=d|m-n|$ for the first integral, $\beta_o=a+d|m-n|$ for the second integral, and $\beta_o=a-d|m-n|$ if $a\geq d|m-n|$ whereas $\beta_o=d|m-n|-a$ if $a<d|m-n|$ for the third integral.

Equation (27) can be evaluated from the following contour integrals:

$$\left\{ \int_{\Gamma} + \int_{-R}^{-(\zeta+\rho)} + \int_{-(\zeta-\rho)}^{+R} \right\} f(z)\, dz = 2\pi i (\text{Res})_{z=i\alpha} + \pi i (\text{Res})_{z=-\zeta} \quad . \quad (28)$$

The residue of $f(z)$ at $z=i\alpha$ is obtained as

$$(\text{Res})_{z=i\alpha} = \frac{1}{(2-1)!} \frac{d}{dz} \{(z-i\alpha)^2 f(z)\}_{z=i\alpha}$$

$$= \frac{-\exp(-\beta_o \alpha)}{4\alpha^3 \{[\alpha(3\zeta^2-\alpha^2)]^2 + [\zeta(z^2-3\alpha^2)]^2\}}$$

$$\times \left[\left\{ \alpha(3\zeta^2-\alpha^2)[\zeta(2\beta_o\alpha+1)\cos(2\beta_o\zeta) - \alpha(2\beta_o\alpha+3)\sin(2\beta_o\zeta)] \right.\right.$$

$$\left. -\zeta(\zeta^2-3\alpha^2)[\alpha(2\beta_o\alpha+3)\cos(2\beta_o\zeta) + \zeta(2\beta_o\alpha+1)\sin(2\beta_o\zeta)] \right\}$$

$$+ i \left\{ \alpha(3\zeta^2-\alpha^2)[\alpha(2\beta_o\alpha+3)\cos(2\beta_o\zeta) - \alpha(2\beta_o\alpha+1)\sin(2\beta_o\zeta)] \right.$$

$$\left.\left. +\zeta(\zeta^2-3\alpha^2)[\zeta(2\beta_o\alpha+1)\cos(2\beta_o\zeta) - \alpha(2\beta_o\alpha+3)\sin(2\beta_o\zeta)] \right\} \right] . \quad (29)$$

The residue of $f(z)$ at $z=-\zeta$ is obtained as

$$(\text{Res})_{z=-\zeta} = \frac{1}{(2-1)!} \frac{d}{dz} \{(z+\zeta)^2 f(z)\}_{z=-\zeta}$$

$$= \frac{2}{(\zeta^2+\alpha^2)^3} \left\{ 2\zeta + i\beta_o(\zeta^2+\alpha^2) \right\} . \quad (30)$$

Since the first integral in equation (28) becomes zero as $R \to \infty$ by Jordan's lemma, equation (28) is written as

$$\lim_{\substack{R\to\infty \\ \rho\to 0}} \int_{-R}^{-(\zeta+\rho)} + \int_{-(\zeta-\rho)}^{+R} f(z)\,dz = \mathrm{Re}\{2\pi i(\mathrm{Res})_{z=i\alpha} + \pi i(\mathrm{Res})_{z=-\zeta}\}$$

$$= 2\pi \Big\{ \exp(-2\beta_o\alpha)\,[\alpha(3\zeta^2-\alpha^2)\{\alpha(2\beta_o\alpha+3)\cos(2\beta_o\zeta) + \zeta(2\beta_o\alpha+1)\sin(2\beta_o\zeta)\}$$

$$+ \zeta(\zeta^2-3\alpha^2)\{\zeta(2\beta_o\alpha+1)\cos(2\beta_o\zeta) - \alpha(2\beta_o\alpha+3)\sin(2\beta_o\zeta)\}]/A - \beta_o/B \Big\}, \qquad (31)$$

where $A = 4\alpha^3\,\{[\alpha(3\zeta^2-\alpha^2)]^2 + [\zeta(\zeta^2-3\alpha^2)]^2\}$ and $B=(\zeta^2+\alpha^2)^2$. If equation (31) is substituted into equation (26), then equation (26) becomes

$$I_2 = \frac{\pi}{a^2 M^2 A B} \sum_{m=1-M}^{M-1} (M-|m|)\, G(d|m|), \qquad (32)$$

where

$$G(d|m|) = B \exp(-2d|m|\alpha)\Big\{ C\,[\alpha(2d|m|\alpha+3)\cos(2d|m|\zeta) + \zeta(2d|m|\alpha+1)\sin(2d|m|\zeta)] + D\,[\zeta(2d|m|\alpha+1)\cos(2d|m|\zeta) - \alpha(2d|m|\alpha+3)\sin(2d|m|\zeta)]\Big\} - A\,d|m|$$

$$- \frac{1}{2} \Big\{ B \exp[-2(a+d|m|)\alpha] \Big[C \Big(\alpha[2(a+d|m|)\alpha+3] \cos[2(a+d|m|)\zeta] + \zeta[2(a+d|m|)\alpha+1] \sin[2(a+d|m|)\zeta] \Big) + D \Big(\zeta[2(a+d|m|)\alpha+1] \cos[2(a+d|m|)\zeta] - \alpha[2(a+d|m|)\alpha+3] \sin[2(a+d|m|)\zeta] \Big) \Big] - A(a+d|m|) \Big\} - g(d|m|), \quad (33)$$

where $C = \alpha(3\zeta^2-\alpha^2)$ and $D = \zeta(\zeta^2-3\alpha^2)$.

The expression for $g(d|m|)$ is given by

$$g(d|m|) = \frac{1}{2} \Big\{ B \exp[-2(a-d|m|)\alpha] \Big[C \Big(\alpha[2(a-d|m|)\alpha+3] \cos[2(a-d|m|)\zeta] + \zeta[2(a-d|m|)\alpha+1] \sin[2(a-d|m|)\zeta] \Big) + D \Big(\zeta[2(a-d|m|)\alpha+1] \cos[2(a-d|m|)\zeta] - \alpha[2(a-d|m|)\alpha+3] \sin[2(a-d|m|)\zeta] \Big) \Big] + A\,(a-d|m|) \Big\} \quad (34)$$

for $a \geq d|m|$, and

$$g(d|m|) = \frac{1}{2} \Big\{ B \exp[-2(d|m|-a)\alpha] \Big[C \Big(\alpha[2(d|m|-a)\alpha+3] \cos[2(d|m|-a)\zeta] + \zeta[2(d|m|-a)\alpha+1] \sin[2(d|m|-a)\zeta] \Big) + D \Big(\zeta[2(d|m|-a)\alpha+1] \cos[2(d|m|-a)\zeta] - \alpha[2(d|m|-a)\alpha+3] \sin[2(d|m|-a)\zeta] \Big) \Big] + A\,(d|m|-a) \Big\} \quad (35)$$

for $a \leq d|m|$.

Similarly, the second integral in equation (22) is obtained as

$$J_2 = \frac{\pi}{2b^2\beta^3N^2} \sum_{n=1-N}^{N-1} (N-|n|)\, G(e|n|) \,, \tag{36}$$

where

$$G(e|n|) = 2(b-e|n|)\beta - \exp(-2e|n|\beta) + \exp(-2b\beta)\cosh(2e|n|\beta) \tag{37}$$

for $b \geq e|n|$, and

$$G(e|n|) = \exp(-2e|n|\beta)\,[\cosh(2b\beta)-1] \tag{38}$$

for $b < e|n|$.

It should be noted that the conditions of $a > d|m|$ (equation (35)) and $b > e|n|$ (equation (38)) represent the cases where the dimensions of each hydrophone exceed the corresponding separations, which implies that adjacent rectangular hydrophones are overlapping in both the x- and y-directions.

The frequency spectral density for a single hydrophone can be calculated using equation (32) with M=1 and equation (36) with N=1 as follows:

$$(I_2)_{M=1} = [\pi/(a^2AB)]\ [\ B\{(3\alpha C+\zeta D) - \exp(-2\alpha a)[\ \{C\alpha(2\alpha a+3)+D\zeta(2\alpha a+1)\}\cos(2\zeta a) + \{C\zeta(2\alpha a+1)-D\alpha(2\alpha a+3)\}\sin(2\zeta a)\ ]\} - Aa\ ],\qquad (39)$$

and

$$(J_2)_{N=1} = [\pi/(2b^2\beta^3)]\ [\ 2b\beta + \exp(-2b\beta) - 1\ ].\qquad (40)$$

NUMERICAL CALCULATIONS AND DISCUSSION

The frequency spectral density for an array of rectangular hydrophones mounted on a rigid surface can be obtained by evaluating equation (1). The integration of equation (1) requires the evaluations of equations (32) and (36). The frequency spectral density is expressed in $dB//\mu Pa^2 Hz^{-1}$. The major results presented in this work are the noise reductions defined as

$$NR = 10 \log_{10} |[Q(\omega)]/[Q(\omega)]_o| \quad dB, \tag{41}$$

where $[Q(\omega)]$ is the frequency spectral density calculated for a given hydrophone array configuration and $[Q(\omega)]_o$ is that calculated for a point hydrophone. The baseline data used in the present study are given below:

$\rho_o = 1.0$ g/cm^3

$c_o = 150{,}000$ cm/s

$U = 20$ knots

$v_* = 0.035\ U.$

The convective flow velocity, u_c, is a function of frequency as shown by Bull[8], and an empirically fitted expression using Bull's measured data is obtained as

$$u_c = U\ [\ 0.6 + 0.4 \exp(-0.8\omega\delta^*/U)], \tag{42}$$

where $\delta^* = 0.35$ cm is the average value of the displacement thicknesses shown in Bull's measurements. As can be seen in equation (42), the convective flow velocity asymptotically approaches the free stream velocity, U, as the frequency decreases, and 0.6 U as the frequency increases.

A recent work by Sherman, Ko, and Buehler[9] has shown that the difference between the peak level (convective ridge) of the turbulent wall pressure spectrum and the level at the low wavenumber region is approximately 35 to 45 dB. This value has been estimated by adjusting the contamination due to the acoustic and flexural wavenumbers at the low wavenumber region. In their study, Martin and Leehey[10] showed that their measurements of low wavenumber wall pressure spectrum are 36 dB below corresponding convective ridge levels.

Case (1) Modified Corcos Model

Based on the work of references 9 and 10, a set of constants that makes the peak-to-low wavenumber ratio 40 dB are determined for use in equation (2) as follows:

$$a_o = 1, \quad \text{(arbitrary scale)}$$
$$c_1 = 0.1,$$
$$c_2 = 1. \qquad (43)$$

The frequency spectral density has been evaluated using equations (32) and (36) for an array of hydrophones and equations (39) and (40) for a single hydrophone. Table 1 shows the calculated results ($dB//\mu Pa^2 Hz^{-1}$) for a flush-mounted point hydrophone and a 10x10 array of 2-in.-square hydrophones with no gaps between adjacent hydrophones. The first column is the frequency in Hz; the second is the point hydrophone result; third is the result calculated using equations (32) and (36); and the fourth is the numerically integrated results via Simpson's rule with range $-5k_c \leq (k_x, k_y) \leq +5k_c$. The last column is the noise reduction, which is the difference between the values of the second and third columns.

Figure 5 presents the effect of the hydrophone dimensions on the noise reduction as a function of frequency for the flow speed of 20 knots. The solid, single chain-dashed, and double chain-dashed lines are the calculated results for 1-, 3- and 10-in.-square hydrophones, respectively. The peaks in the curves correspond to locations where the convective ridge wavenumber is aligned with the hydrophone sidelobe level peak. Conversely, nulls in the noise reduction curves correspond to the convective ridge wavenumber aligned with hydrophone beam pattern nulls. However, it is shown that the peaks and valleys corresponding to narrow sidelobes in the hydrophone response diminishes as the hydrophone becomes larger. As can be seen in the figure, more noise is attenuated as the size of the hydrophone increases.

Figure 6 shows the effect of the number of 2-in.-square hydrophone array elements on noise reduction as a function of frequency for the flow speed of 20 knots. These results are for the case of no gaps between adjacent hydrophones. It is seen in the figure that as the number of array elements increases, more noise is eliminated. The peaks in the low frequency region correspond to locations where the convective ridge wavenumber is aligned with the array aliasing lobe level peaks. Conversely, nulls in the noise reduction curves correspond to the convective ridge wavenumber aligned with array beam pattern nulls. However, it is shown that the peaks and valleys corresponding to narrow sidelobes in the array response diminish as the number of array elements increases. Figure 7 shows the results of a 2-in.-square hydrophone array for the case of 1-in. gaps between adjacent hydrophones.

Case (2) (Original Corcos Model)

The original Corcos model is given as follows:[8,11]

$$P(k_x,k_y,\omega) = \frac{a_o\ \rho_o^2\ v_*^4}{\omega\ \pi^2} \left\{\frac{\alpha_1 k_c}{(k_x-k_c)^2+\ (\alpha_1 k_c)^2}\right\} \left\{\frac{\alpha_2 k_c}{k_y^2+(\alpha_2 k_c)^2}\right\}, \qquad (44)$$

where $k_c=\omega/u_c$, and a_o, α_1, and α_2 are the constants to be determined. Based on the work of references 9 and 10, a set of constants that makes the peak-to-low wavenumber ratio 40 dB are

determined for use in equation (43) as follows:

$$a_o = 1, \quad \text{(arbitrary scale)}$$
$$\alpha_1 = 0.01,$$
$$\alpha_2 = 1. \tag{45}$$

The above constants have been utilized by Ko and Schloemer[3] in their study of the response of an array of hydrophones embedded in an elastomer layer to a modified Corcos turbulent wall pressure spectrum. The modified Corcos model in reference 3 is not the same as that in reference 4. The term "modified" is used only to distinguish the Corcos model with constants determined by Chase[7]. The constants shown in reference 7 are as follows:

$$a_o = a_+ (1+\gamma) \simeq 1$$
$$a_+ = 0.766,$$
$$\gamma = 0.389,$$
$$\alpha_1 = 0.09,$$
$$\alpha_2 = 7\alpha_1. \tag{46}$$

It should be noted that the above constants give a peak-to-low wavenumber ratio of 21 dB. These constants have been used by Ko and Nuttall[1] in their study of the analytical evaluation of flush-mounted hydrophone array response to the Corcos turbulent wall pressure spectrum. The results calculated using the constants given by equation (46) are presented in table

1 of reference 1. Note that the convective velocity used in reference 1 is $u_c = 0.6\ U$.

Table 2 shows the results calculated using the constants given by equation (45). The results presented in table 2 have been obtained from equations (50) and (53) in reference 1 for an array of hydrophones and from equations (28) and (29) in reference 1 for a single hydrophone, with the constants given by equation (45). Figure 8 shows the effect of the hydrophone dimensions on the noise reduction. The mean flow speed is 20 knots. The solid, single chain-dashed, and double-dashed lines are the calculated results for 1-, 3- and 10- in.-square hydrophones, respectively. The peaks in the curves correspond to locations where the convective ridge wavenumber is aligned with the hydrophone sidelobe level peak. Conversely, nulls in the noise reduction curves correspond to the convective ridge wavenumber aligned with hydrophone beam pattern nulls. However, it is shown that the peaks and valleys corresponding to narrow sidelobes in the hydrophone response diminish as the hydrophone becomes larger. As can be seen in the figure, more noise is attenuated as the size of the hydrophone increases.

Figure 9 shows the effect of the number of 2-in.-square hydrophone array elements on noise reduction as a function of frequency for the flow speed of 20 knots. These results are for the case of no gaps between adjacent hydrophones. It is seen in the figure that as the number of array elements increases, more

noise is eliminated. The peaks in the low frequency region correspond to locations where the convective ridge wavenumber is aligned with the array aliasing lobe level peaks. Conversely, nulls in the noise reduction curves correspond to the convective ridge wavenumber aligned with array beam pattern nulls. However, it is shown that the peaks and valleys diminish as the number of array elements increases, corresponding to narrow sidelobes in the array response. Figure 10 shows the results of 2-in.-square hydrophone array for the case of 1-in. gaps between adjacent hydrophones.

Case (3) Comparison

Figure 11 shows a comparison between the results calculated using the original Corcos model (equation (43) with constants given by equation (45)) and the modified Corcos model (equation (2) with constants given by equation (43)) for a 2-in.-square hydrophone. Figure 12 shows a comparison between the results calculated for the 10x10 array of 2-in.-square hydrophones with no gaps between adjacent hydrophones. The solid and dashed lines are the results calculated for the original and modified Corcos models, respectively. As shown in the figure, the results calculated for two different models are very close to each other for the low frequency region. However, as shown in figures 11 and 12, the results calculated using the original Corcos model

show less noise reductions compared with those calculated using the modified Corcos model.

Summary

In this study, the calculated results for a modified Corcos model with constants given by equation (43) and the original Corcos model with equation (45) are presented for comparison; they are found to be in good agreement as shown in figures 11 and 12 for the low frequency region. Therefore, the original Corcos model adjusted to the peak-to-low wavenumber ratio of 40 dB is recommended in lieu of the modified Corcos model for use in the calculation of the frequency spectral density for low frequency. However, the question of how to develop a proper flow excitation function still remains unanswered for the reduction of turbulent boundary layer pressure fluctuations. Many fundamental questions regarding extremely complicated turbulence structures are to be answered before an adequate turbulent wall pressure model is fully accepted. In conclusion, the original Corcos model shown in equation (44) is an expression that shows reasonable performance in the low frequency range when the empirically determined constants α_1=0.01 and α_2=1 are employed.

CONCLUSIONS

An investigation has been made for predictions of the flow noise level received by an array of rectangular hydrophones flush-mounted on a rigid surface. The hydrophone array mounted on the surface is exposed to turbulent flow. In the present work, an array of hydrophones is flush-mounted on a rigid surface and is exposed to turbulent flow. Major results presented in this study are the turbulent noise reductions.

° The frequency spectral density that represents the hydrophone array response is obtained by evaluating the double integral shown in equation (1). In the present study, the double integral is reduced to the product of two single integrals. The two single integrals have been evaluated by using the contour integral method (residue method).

° It is found that more noise is attenuated as (1) the number of array elements increases, and (2) the hydrophone dimensions increase. The array configuration with no gaps between adjacent hydrophones provides more noise attenuation than that with gaps between adjacent hydrophones for the low frequency region.

° It is found that the results calculated for the original and modified Corcos models are very close to each other when the wall pressure spectrum has the peak-to-low wavenumber ratio of 40 dB. It is anticipated that the original Corcos model with α_1=0.01,

and α_2=1 (in lieu of α_1=0.09 and α_2=0.63) would be an acceptable excitation function for use in the flow noise prediction.

° It should be remembered that the peaks and valleys in noise reduction curves will not appear when a hydrophone or an array of hydrophones are covered by a layer of elastomer. This can be accomplished by following the procedures described in reference 4.

° This work provides a tool for the quick estimate on the response of an array of hydrophones to turbulent boundary layer pressure fluctuations. The analytical expressions shown in both the present work and reference 1 can be conveniently programmed using a desk-top computer.

° In summary, the original Corcos model shown in equation (44) with constants given by equation (45) is an empirical expression that shows a reasonable performance when the frequency spectral density is calculated. Therefore, the original Corcos model adjusted to the peak-to-low ratio of 40 dB is recommended for low frequency ranges in lieu of the modified Corcos model for use in the prediction of the frequency spectral density.

REFERENCES

1. S. H. Ko and A. H. Nuttall, "Analytical Evaluation of Flush-Mounted Hydrophone Array Response to the Corcos Turbulent Wall Pressure Spectrum," Journal of the Acoustical Society of America, Vol. 90, No. 1 (1991)

2. W. Thompson, "The Rapid Evaluation of Two-Dimensional Power Spectral Density Integrals for Large Arrays of Rectangular Sensors Excited by Turbulent Flow," Applied Research Laboratory, Pennsylvania State University, Technical Memorandum File No. 89-191 (29 March 1990)

3. S. H. Ko and H. H. Schloemer, "Calculations of Turbulent Boundary Layer Pressure Fluctuations Transmitted into a Viscoelastic Layer." Journal of the Acoustical Society of America, Vol. 85, No. 4 (1989)

4. S. H. Ko and H. H. Schloemer, "Response of an Array of Hydrophones Embedded in an Elastomer Layer to a Modified Corcos Turbulent Wall Pressure Spectrum." Paper presented at the 120th Meeting of the Acoustical Society of America, 26-30 November 1990, San Diego, CA.

5. R. C. Elswick (Personal Communication 1983)

6. H. Schlichting, Boundary Layer Theory, McGraw-Hill, New York 1968, p.602.

7. D. M. Chase, "The Modelling of the Wave-Vector Frequency Spectrum of Turbulent Boundary Wall Pressure," Journal of Sound and Vibration, Vol. 70 (1980)

8. M. K. Bull, "Wall-Pressure Fluctuations Associated with Subsonic Turbulent Boundary Layer Flow," Journal of Fluid Mechanics, Vol. 28 (1967)

9. C. H. Sherman, S. H. Ko, and B. G. Buehler, "Measurement of the Turbulent Boundary Layer of Wave-Vector Spectrum," Journal of Acoustical Society of America, Vol. 88 (1990)

10. M. C. Martin and P. Leehey, "Low Wavenumber Wall Pressure Measurements Using a Rectangular Membrane as a Spatial Filter," Journal of Sound and Vibration, Vol. 52 (1977)

11. G. M. Corcos, "The Structure of the Turbulent Pressure Field in Boundary Layer Flows," Journal of Fluid Mechanics, Vol. 18 (1964)

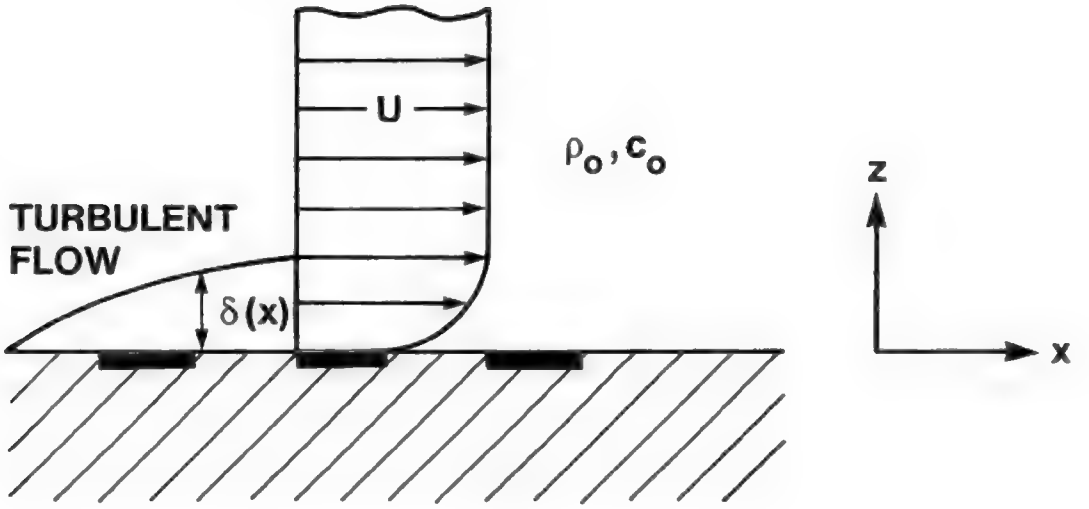

Figure 1. Theoretical Model

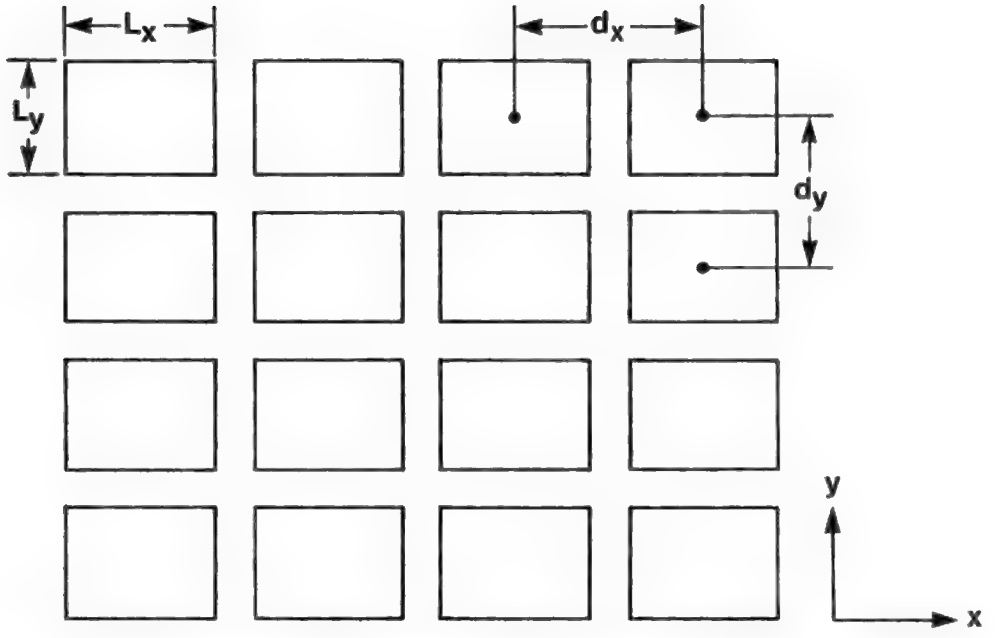

Figure 2 Configuration of Hydrophone Array

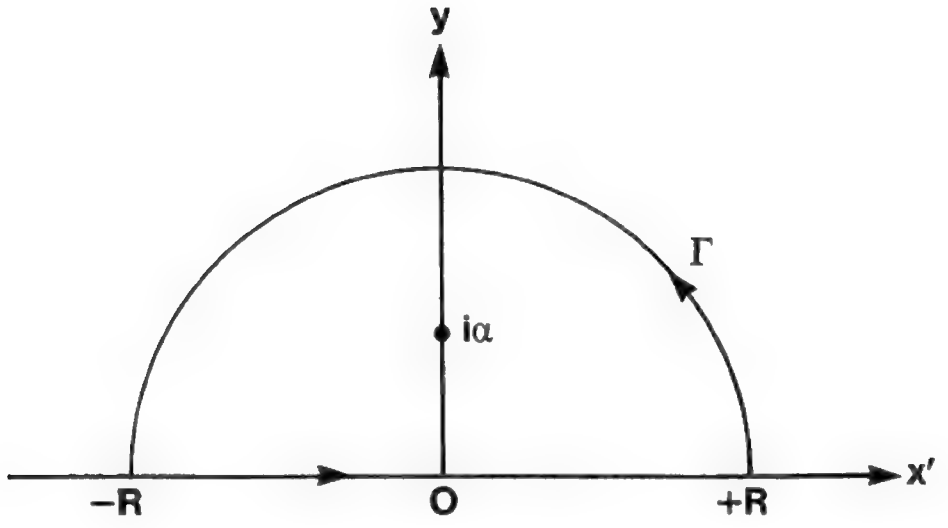

Figure 3 Contour of Integration (No poles on the Real Axis) in the Complex z-Plane

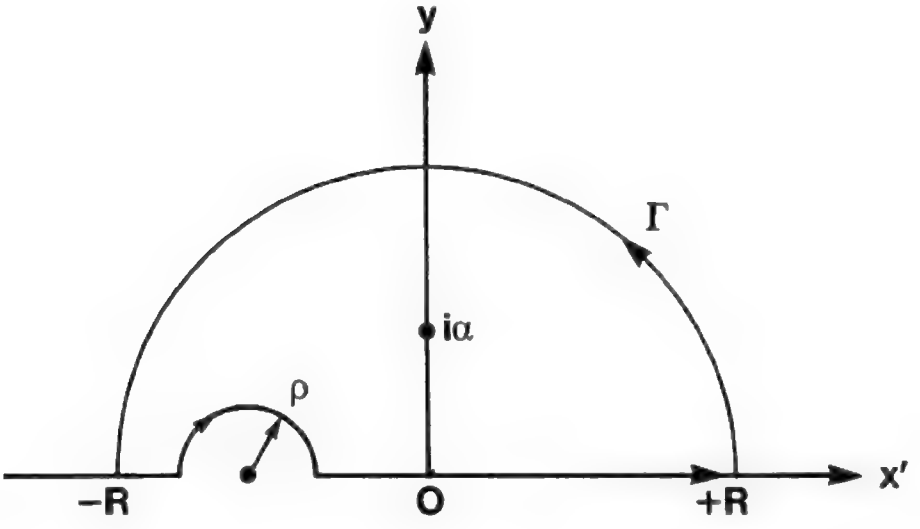

Figure 4 Contour of Integration (Poles on the Real Axis) in the Complex z-Plane

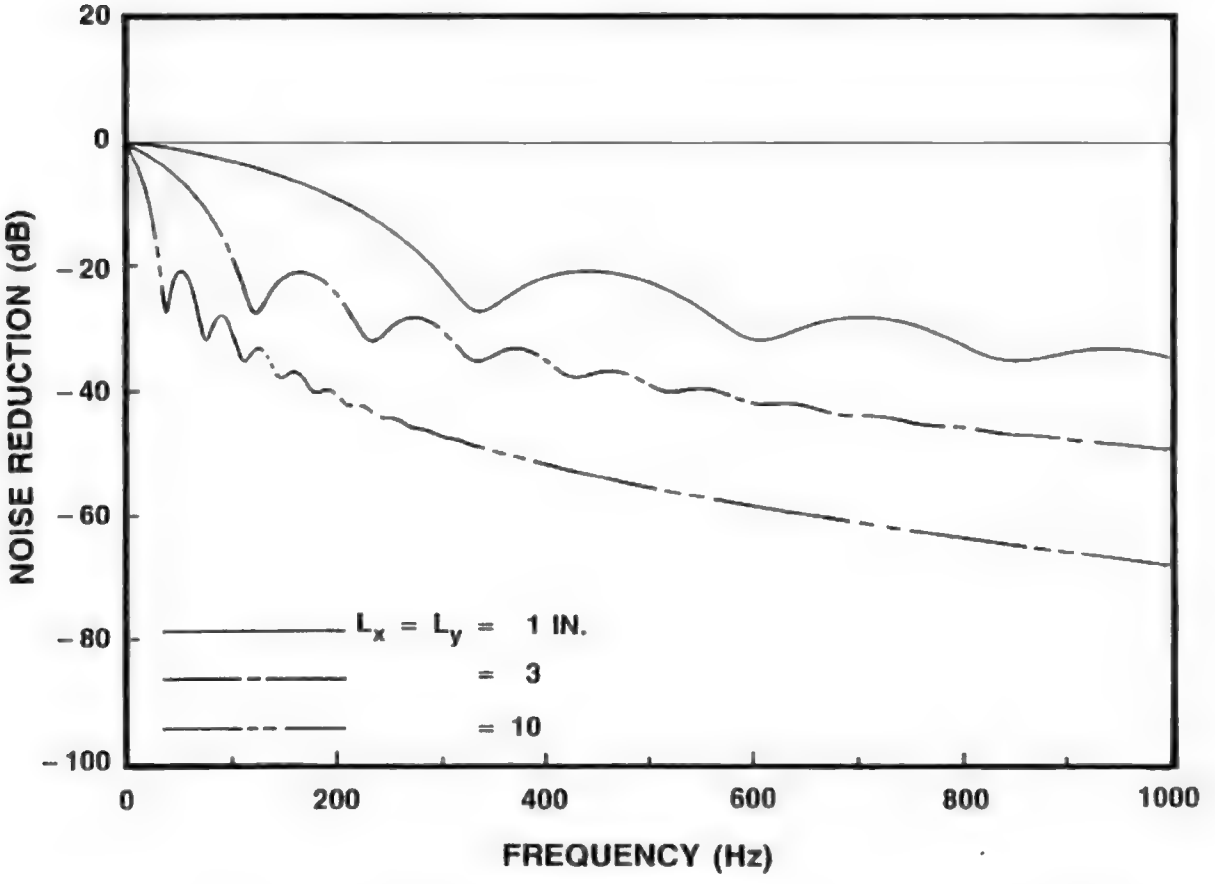

Figure 5 Effect of the Dimensions of a Hydrophone on the Flow Noise Reduction (Modified Corcos Model)

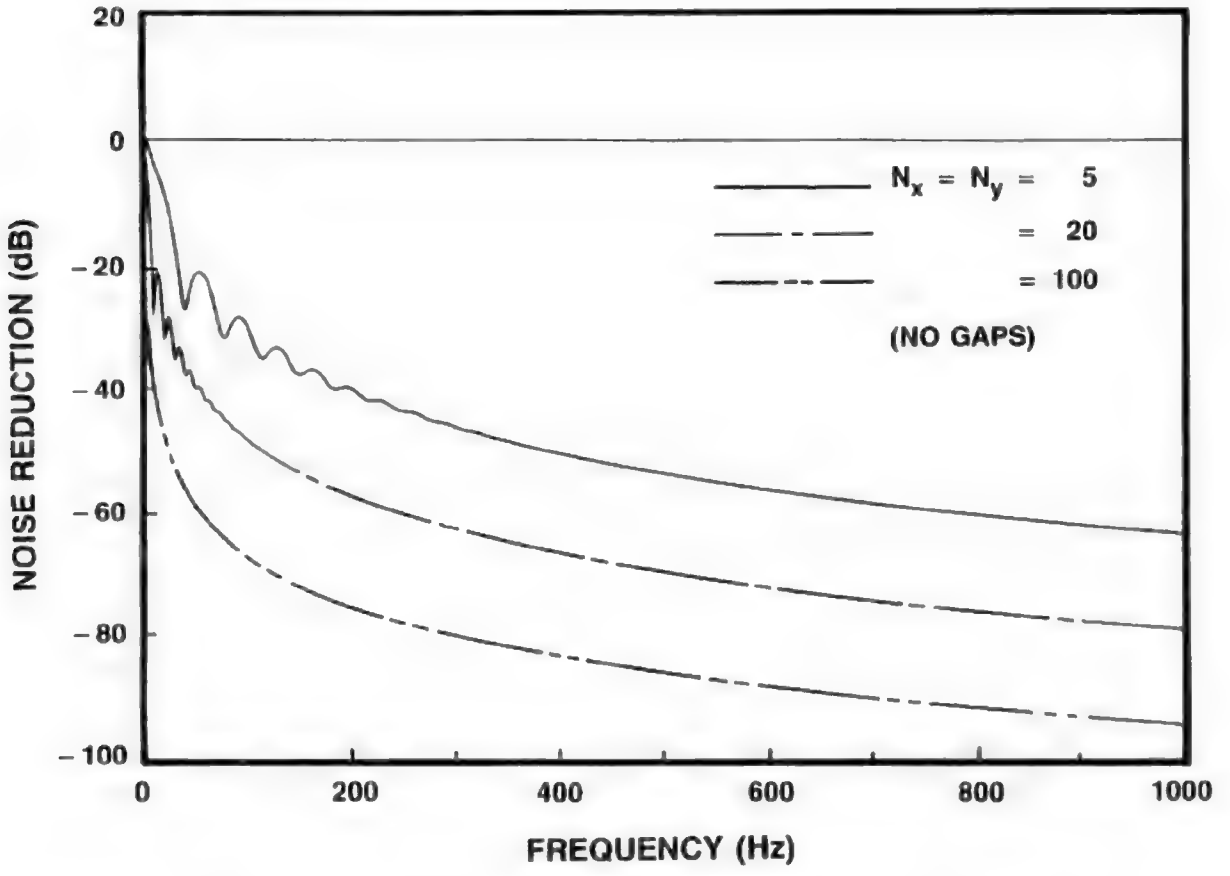

Figure 6 Effect of the Number of Square Hydrophone Array Elements (No Gaps between Hydrophones) on the Flow Noise Reduction (Modified Corcos Model)

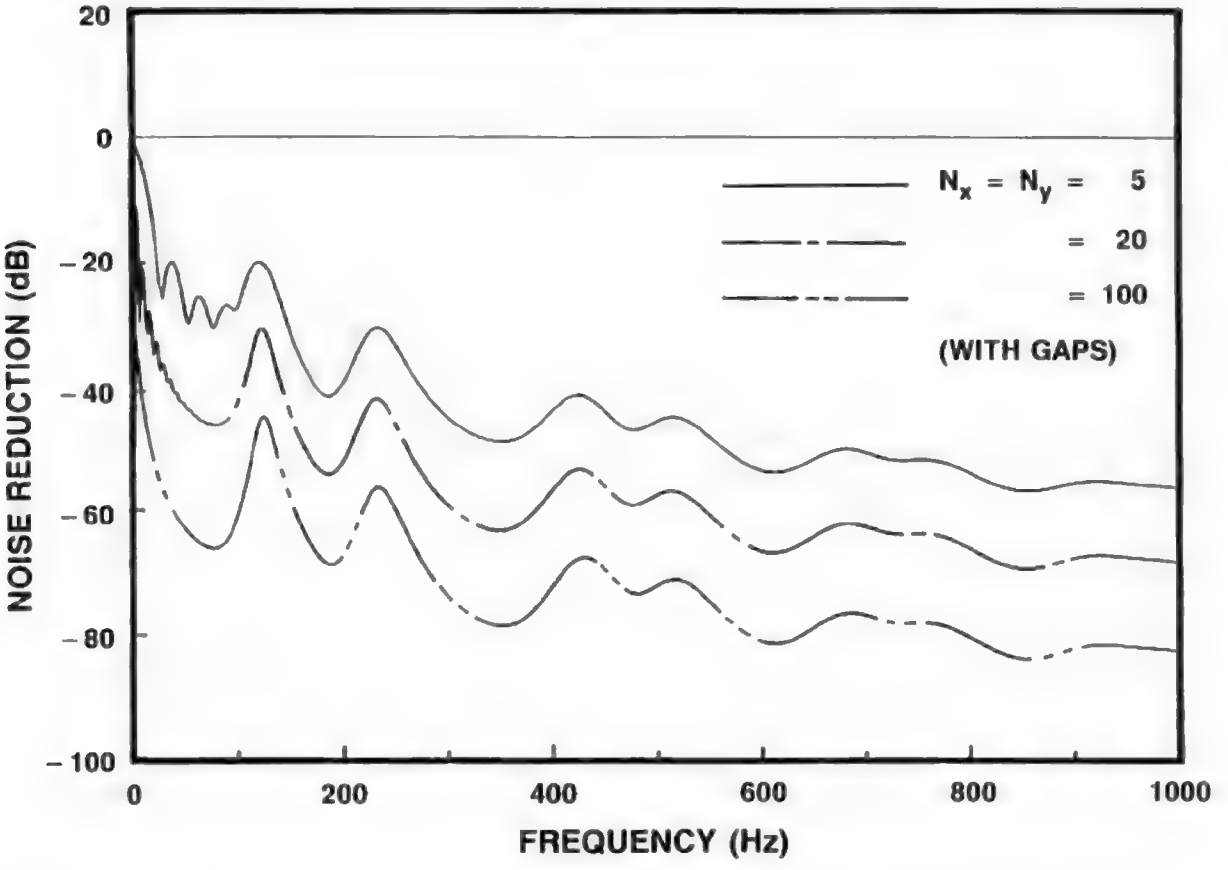

Figure 7 Effect of the Number of Square Hydrophone Array Elements (Gaps between Hydrophones) on the Flow Noise Reduction (Modified Corcos Model)

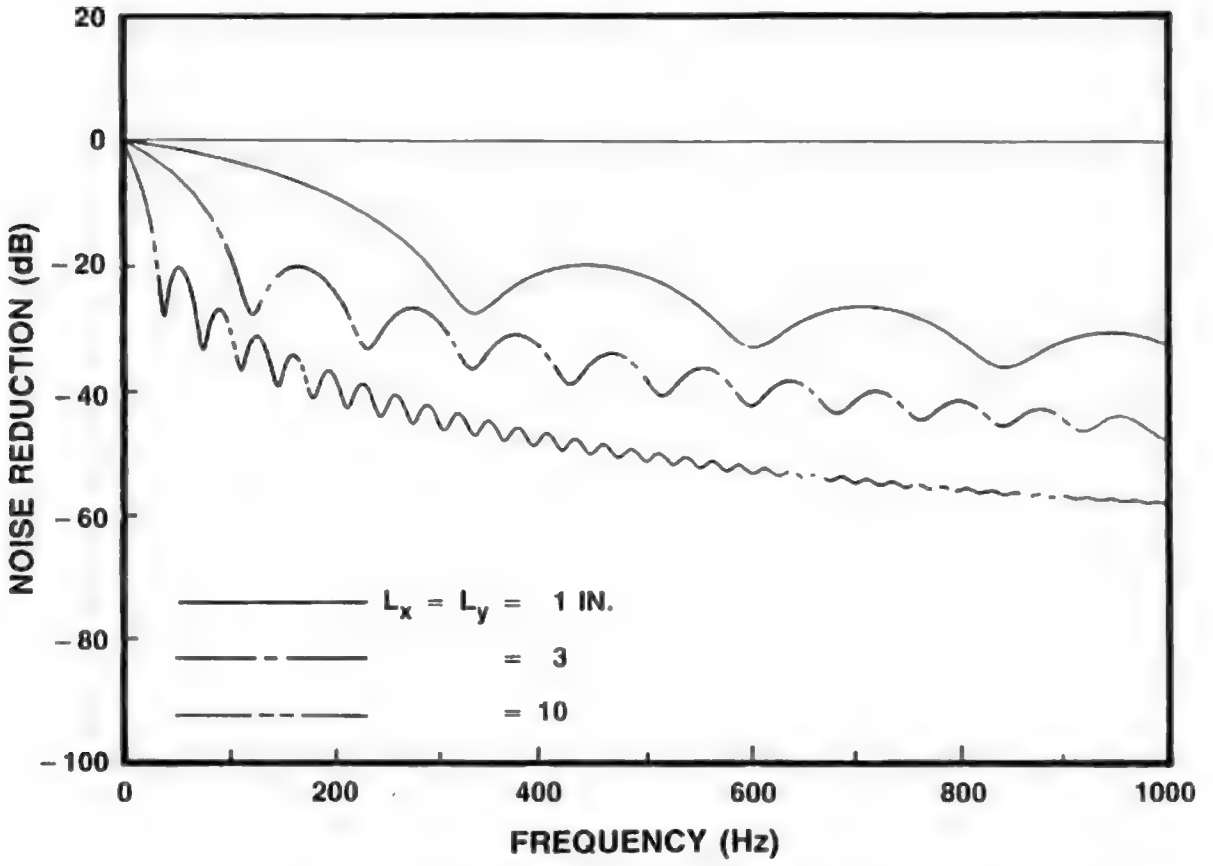

Figure 8 Effect of the Dimensions of a Hydrophone on the Flow Noise Reduction (Original Corcos Model)

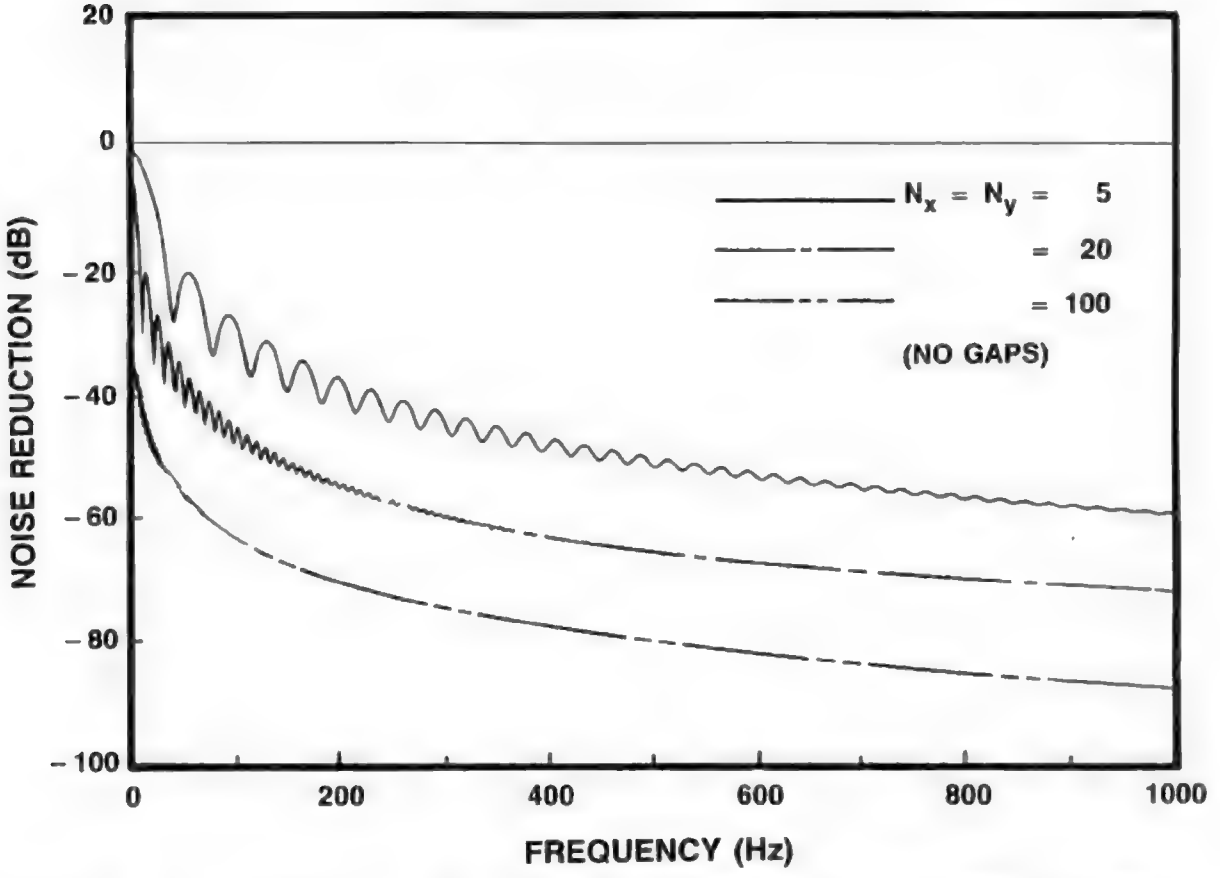

Figure 9 Effect of the Number of Square Hydrophone Array Elements (No Gaps between Hydrophones) on the Flow Noise Reduction (Original Corcos Model)

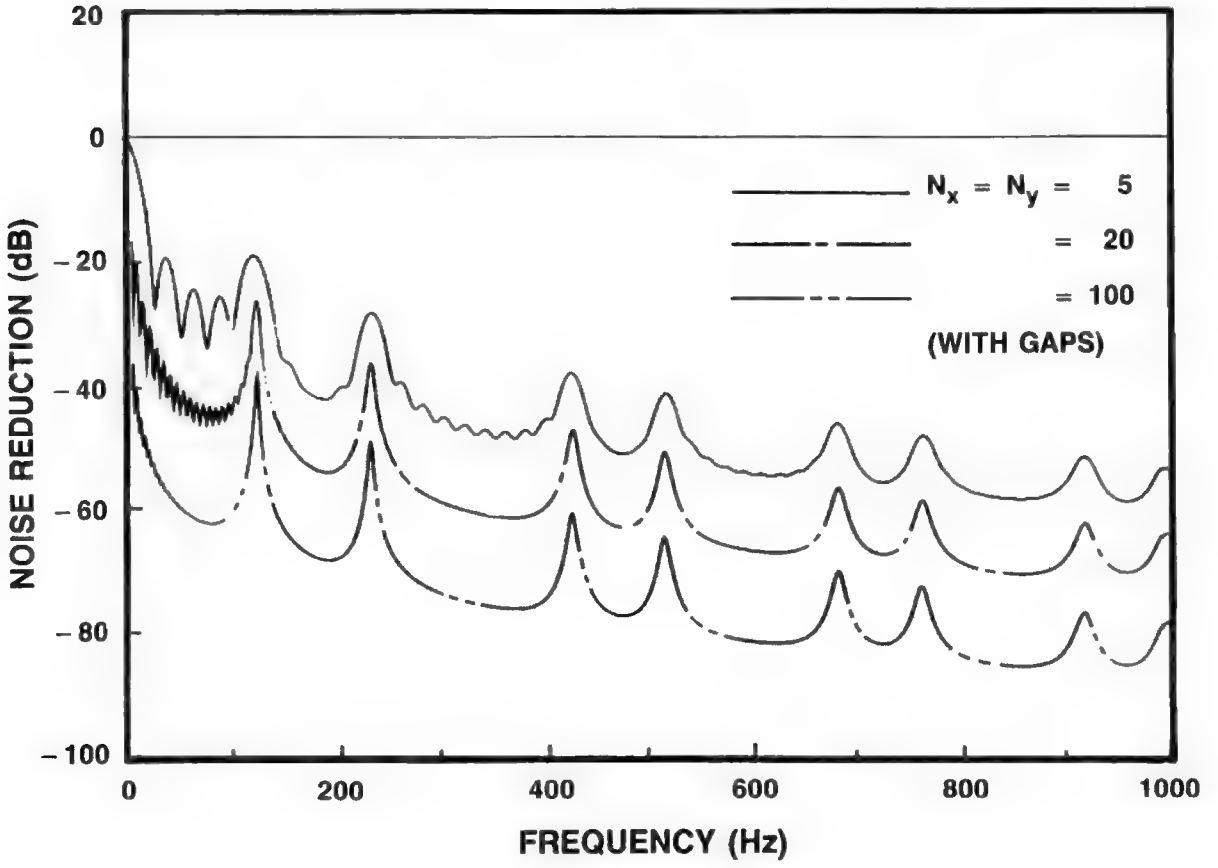

Figure 10 Effect of the Number of Square Hydrophone Array Elements (Gaps between Hydrophones) on the Flow Noise Reduction (Original Corcos Model)

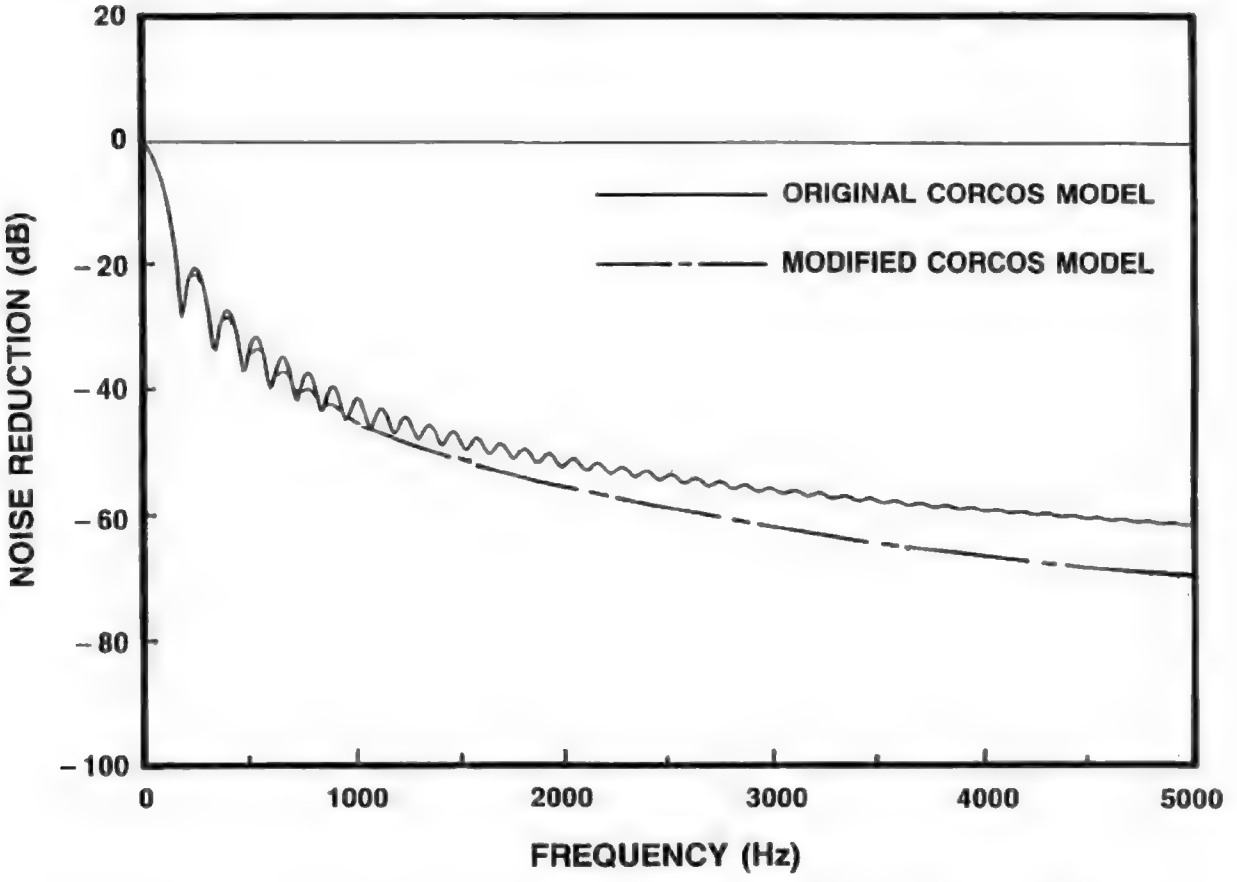

Figure 11 Comparison between the Results Calculated using the Original and Modified Corcos Models for a 2-in.-Square Hydrophone

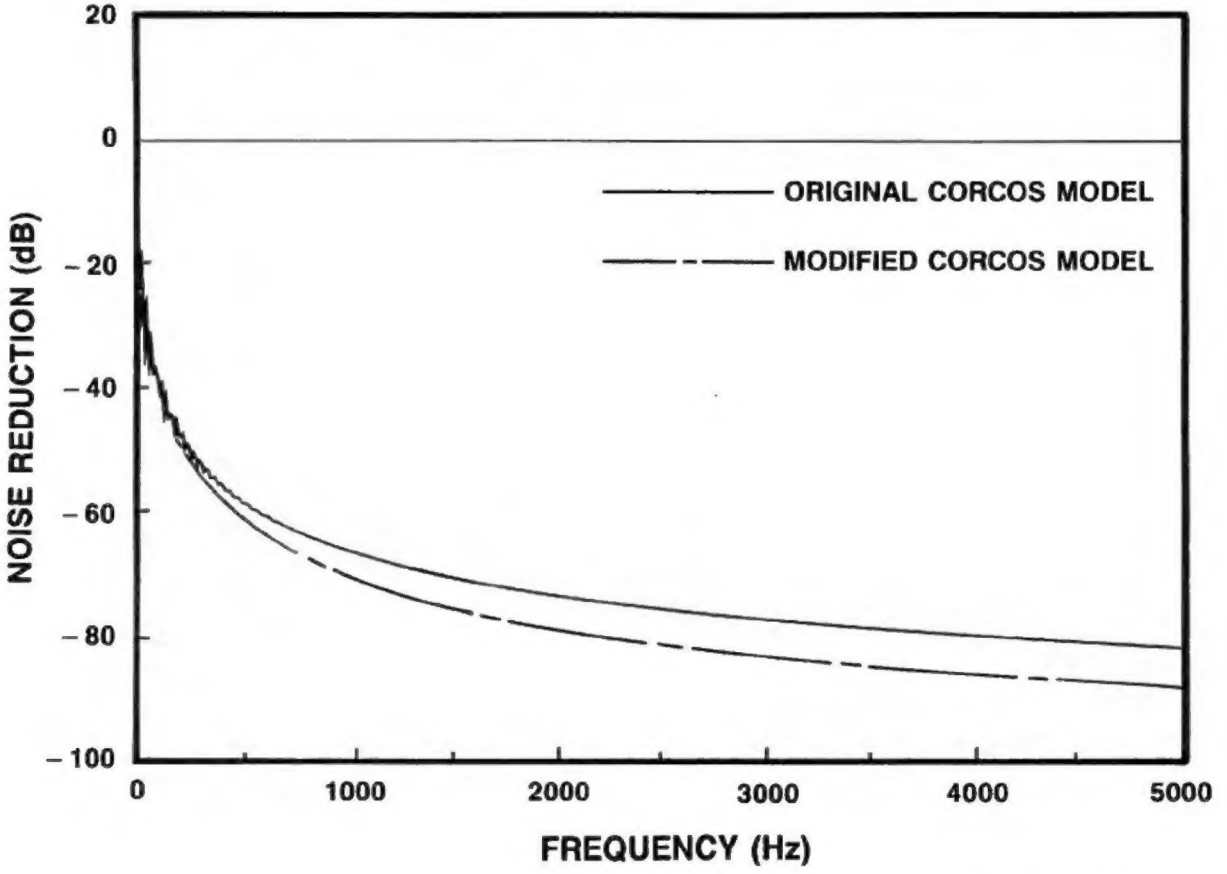

Figure 12 Comparison between the Results Calculated using the Original and Modified Corcos Models for the 10x10 Array of 2-in.-Square Hydrophones

Table 1. Calculated frequency spectral densities for a 10 x 10 array of 2-in.-square hydrophones with no gaps between adjacent hydrophones and for a point hydrophone (Modified Corcos model with $c_1 = 0.1$ and $c_2 = 1.0$)

Frequency (Hz)	Point hydrophone dB//$\mu Pa^2 Hz^{-1}$	Analytical expression dB//$\mu Pa^2 Hz^{-1}$	Numerical integration dB//$\mu Pa^2 Hz^{-1}$	Noise reduction (dB)
100	142.5286	102.91450	102.91430	- 39.34481
200	139.5183	90.47374	90.47364	- 48.77530
300	137.7574	83.08268	83.08262	- 54.40544
400	136.5080	77.78826	77.78821	- 58.45048
500	135.5389	73.68091	73.68087	- 61.58873
600	134.7471	70.34100	70.34097	- 64.13683
700	134.0777	67.54104	67.54101	- 66.26732
800	133.4977	65.14251	65.14249	- 68.08593
900	132.9862	63.05415	63.05413	- 69.66277
1000	132.5286	61.21226	61.21224	- 71.04708
1100	132.1147	59.57048	59.57047	- 72.27493
1200	131.7368	58.09392	58.09391	- 73.37360
1300	131.3892	56.75563	56.75562	- 74.36427
1400	131.0674	55.53439	55.53438	- 75.26367
1500	130.7677	54.41319	54.41318	- 76.08523
1600	130.4874	53.37823	53.37822	- 76.83991
1700	130.2242	52.41815	52.41814	- 77.53670
1800	129.9759	51.52355	51.52355	- 78.18306
1900	129.7411	50.68657	50.68656	- 78.78523
2000	129.5183	49.90055	49.90054	- 79.34849

Table 2. Calculated frequency spectral densities for a 10 x 10 array of 2-in.-square hydrophones with no gaps between adjacent hydrophones and for a point hydrophone (Original Corcos model with $\alpha_1 = 0.01$ and $\alpha_2 = 1.0$)

Frequency (Hz)	Point hydrophone dB//$\mu Pa^2 Hz^{-1}$	Analytical expression dB//$\mu Pa^2 Hz^{-1}$	Numerical integration dB//$\mu Pa^2 Hz^{-1}$	Noise reduction (dB)
100	142.5286	104.00510	104.00480	- 38.25428
200	139.5183	91.42717	91.42701	- 47.82187
300	137.7574	85.78282	85.78272	- 51.70530
400	136.5080	80.85490	80.85482	- 55.38384
500	135.5389	76.75074	76.75067	- 58.51890
600	134.7471	73.91292	73.91287	- 60.56490
700	134.0777	71.43211	71.43207	- 62.37624
800	133.4977	69.35165	69.35161	- 63.87679
900	132.9862	67.48494	67.48491	- 65.23197
1000	132.5286	65.84829	65.84826	- 66.41105
1100	132.1147	64.36728	64.36725	- 67.47813
1200	131.7368	63.03924	63.03921	- 68.42829
1300	131.3892	61.83305	61.83303	- 69.28685
1400	131.0674	60.72741	60.72739	- 70.07065
1500	130.7677	59.70817	59.70815	- 70.79026
1600	130.4874	58.76425	58.76423	- 71.45389
1700	130.2242	57.88625	57.88623	- 72.06860
1800	129.9759	57.06590	57.06589	- 72.64071
1900	129.7411	56.29619	56.29618	- 73.17561
2000	129.5183	55.57146	55.57144	- 73.67758

TR 8943

DISTRIBUTION LIST

External

NAVSEA (Code 06URB)

DTRC
Dr. William K. Blake (Code 1905)
Dr. Y. F. Hwang (1942)
Dr. G. Maidanik (1902)
Dr. P. Shang (1942)

NRL/Orlando
Dr. J. Blue
Dr. R. Timme
Dr. A. L. Van Buren

ONR
Dr. A. J. Tucker (code 1132)

Penn. State University (ARL)
Dr. C. Burroughs
Dr. G. Lauchle
Dr. W. Thompson

Chase, Inc.
Dr. D. Chase

MIT
Dr. P. Leehey